Thiophene derivatives as effective inhibitors for the corrosion of steel in 0.5 M H$_2$SO$_4$

M. BOUKLAH[1], B. HAMMOUTI[1,*], M. BENKADDOUR[1] and T. BENHADDA[2]

[1]*Laboratoire de Chimie des Eaux et Corrosion, Faculté des Sciences, Université Mohammed 1er, Oujda, Morocco*
[2]*Laboratoire de Chimie d'Activation Moléculaire, Faculté des Sciences, Université Mohammed 1er, Oujda, Morocco*
(*author for correspondence, e-mail: hammoutib@yahoo.fr)

Abstract

The influence of thiophene and five of its substituted derivatives on the corrosion inhibition of steel in 0.5 M H$_2$SO$_4$ solution was studied using weight-loss, electrochemical polarisation, and impedance measurements. 5-tert-butoxythiophene-2-carbaldehyde phenylhydrazone (TBCP) is the best inhibitor and its inhibition efficiency increases with increase in concentration to attain 87% at 5×10^{-3} M. Potentiodynamic polarisation studies clearly reveal that it acts essentially as a cathodic inhibitor. The partial π-charge on atoms has been calculated. A correlation between the highest occupied molecular orbital E_{HOMO} and inhibition efficiencies was sought. The inhibition efficiency of TBCP is not affected by rise in temperature in the range 298–353 K. $E\%$ values obtained from weight-loss and electrochemical methods were in good agreement. Adsorption of TBCP on steel has an S-shaped adsorption isotherm.

1. Introduction

Sulphuric and hydrochloric are the most commonly used acids in pickling baths at high temperatures up to 60 °C. To remove unwanted scale such as rust or mill scale formed during manufacture, carbon steel is immersed in an acid solution. During pickling, corrosion inhibitors are added to the solution in order to reduce the degree of metal attack and rate of acid consumption [1–5]. The role of inhibitors is to form a barrier of one or several molecular layers against acid attack. This protective action is often associated with chemical and/or physical adsorption involving a variation in the charge of the adsorbed substance and transfer of charge from one phase to the other. Most of the efficient acid inhibitors are organic compounds containing mainly nitrogen, sulphur or oxygen atoms in their structure. The inhibition efficiency should follow the sequence O < N < S < P [6–8]. Sulphur and/or nitrogen containing heterocyclic compounds with various substituents are considered to be effective corrosion inhibitors. Thiophene, hydrazine derivatives offer special affinity to inhibit corrosion of metals in acid solutions [9–19].

In continuation of our work on development of new organic compounds as acid inhibitors and the encouraging results obtained by thiophene derivatives [20–22], two organic inhibitors namely 5-*tert*-butoxythiophene-2-carbaldehyde phenylhydrazone (TBCP) and 5-*tert*-butoxythiophene-2-carboxylic acid (TBCA)

have been synthesised and tested as inhibitors of steel corrosion in 0.5 M H$_2$SO$_4$. Their effects were compared to thiophene (T) and other commercial substituted thiophenes. The objective of this work is to study the effect of these thiophene compounds on steel corrosion by using gravimetric and electrochemical polarisation methods. The relation between efficiency and molecular structure is explained using the PETRA program which permits the calculation of the partial π-charge on atoms and quantum chemical indices. The effect of temperature is also evaluated between 298 and 353 K.

2. Experimental details

2.1. *Inhibitors*

Thiophene compounds (T, TM, MTC and ETC) were commercial products. TBCA and TBCP were synthesised, purified and characterised by NMR, IR spectroscopy and element analysis before use. The molecular structures of the thiophenes studied are shown in Figure 1.

2.2. *Gravimetric and polarisation measurements*

Prior to all measurements, the steel samples (0.09%P; 0.38%Si; 0.01%Al; 0.05%Mn; 0.21%C; 0.05%S and the
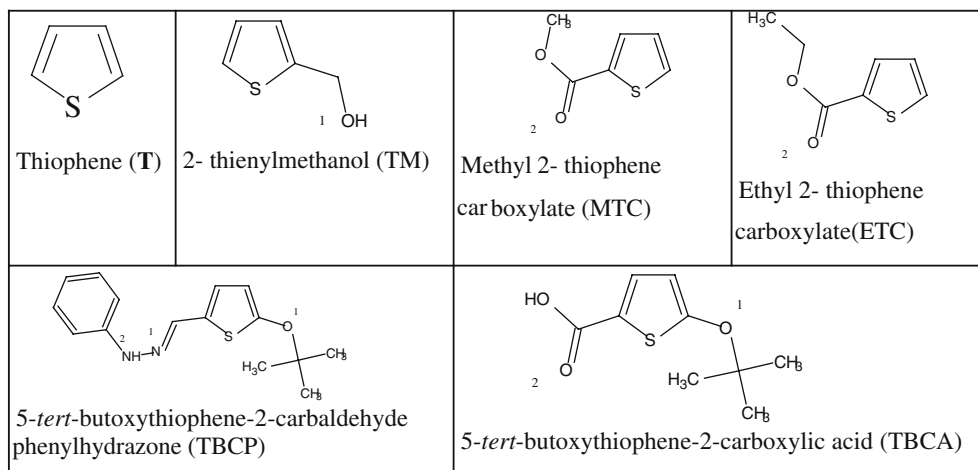
Fig. 1. Thiophene compounds studied.

remainder iron) were polished with emery paper up to 1200 grade, washed thoroughly with bidistilled water degreased and dried with acetone.

The acid solution (0.5 M H_2SO_4) was prepared by dilution of Analytical Grade 98% H_2SO_4 with double distilled water. All tests were conducted at different temperatures in magnetically stirred solutions.

Gravimetric measurements were carried out in a double walled glass cell equipped with a thermostated cooling condenser. The solution volume was 100 cm³. The steel specimens used had a rectangular form (2 cm×2 cm×0.05 cm). These sheets were abraded successively with fine emery paper and then rinsed with distilled water, degreased and dried before being weighed and immersed in the corrosive medium. The immersion time for the weight loss is 6 h at 298 K.

The PETRA program was used to calculate the effect of each substituent on resonance structure and the heteroatoms charge delocalisation process [23].

Electrochemical measurements were carried out in a conventional three-electrode electrolysis cylindrical Pyrex glass cell. The working electrode had the form of a disc cut form steel sheet. The exposed area to the corrosive solution was 1 cm². A saturated calomel electrode (SCE) and a platinum electrode were used, respectively as reference and auxiliary electrodes. Running on an IBM compatible personal computer, the 352 Soft Corr™ III Software communicated with EG&G Instruments potentiostat–galvanostat model 263A at a scan rate of 20 mV min⁻¹. Before recording the cathodic polarisation curves, the steel electrode was polarised at −800 mV for 10 min. For anodic curves, the potential of the electrode was swept from its corrosion potential after 30 min at the free corrosion potential, to more positive values. The test solution was de-aerated with pure nitrogen. Gas bubbling was maintained throughout the experiments. Near E_{corr} a scan through a potential range performs polarisation resistance measurements. All potentials are given on the SCE scale. The cell was thermostated at 298 ± 0.5 K.

The inhibition efficiency E_w was determined from weight loss data by the following relation:

$$E_w\% = \left(1 - \frac{W_{corr}}{W^0_{corr}}\right) \cdot 100$$

where W_{corr} and W^0_{corr} are the corrosion rates of steel with and without TBCP, respectively. For electrochemical measurements, the inhibition efficiency is calculated as follows:

$$E_I\% = \left(1 - \frac{I_{corr}}{I^0_{corr}}\right) \cdot 100$$

where I_{corr} and I^0_{corr} are the corrosion current density values with and without inhibitor, respectively, determined by extrapolation of cathodic Tafel lines to the corrosion potential.

3. Results and discussion

3.1. Comparative study

The effect of addition of tested thiophene compounds at 10^{-3} M on the corrosion of steel in 0.5 M H_2SO_4 was studied by weight-loss at 298 K after 6 h of immersion. Table 1 collects the corresponding values of corrosion rates and inhibition efficiency.

Table 1. Steel weight loss data and corresponding inhibition efficiency of thiophenes at 298 K

Compound	W/mg cm⁻² h⁻¹	E_w/%
0.5 M H_2SO_4	1.608	–
10^{-3} M T	1.126	30
10^{-3} M TM	1.415	12
10^{-3} M MTC	2.042	−27
10^{-3} M ETC	1.785	−11
10^{-3} M TBCA	1.013	37
10^{-3} M TBCP	0.273	83

The variation in inhibitive or catalytic effect mainly depends on the type and nature of the substituents present in the inhibitor molecule. T, TM, TBCA have a weak inhibitory effect and MTC and ETC have a catalytic action on the corrosion process. A high inhibiting effect (83%) is obtained with TBCP.

It seems that the compounds MTC and ETC exist in their acid form in 0.5 M H_2SO_4. Their catalytic effect is inversed when the ter-butoxy group replaces hydrogen hence the efficiency passes from negative to positive values (37%). The higher inhibitory action of TBCP when compared to TBCA may also be explained by the replacement of a carboxylic acid group by a phenyl hydrazinyl group.

To get more information, partial atomic charges in the π-thiophene systems were calculated by generating all valence bond (resonance) structures for this system and then weighting them on the basis of π-orbital electronegativities and formal considerations (PEPE = Partial Equalisation of π-electronegativity) [23].

The charge is moved along the thiophene π-system to the atoms of the resonance structures thereby changing their electronegativity. Therefore, the process of weighting the structures and shifting electron density has to be repeated in several cycles with decreasing amounts of charge being shifted. So the π-charges calculated by the PEPE method for various inhibitors containing N, S and O atoms were correlated with inhibition values as shown in Table 2.

T and TM compounds show similar π-charge for the S atom (0.00 e). However the non-substituted thiophene T is more effective than the 2-hydroxymethyl thiophene TM. This behaviour may be attributed to the S...H–O spatial interaction.

The substitution of hydrogen by the carboxylic group (CO_2R, R = Me or Et) did not improve the degree of inhibition because of the positive charge of the S atom at the 1-position of ETC and MTC which was 0.0173 and 0.0285 e, respectively and O(2) atoms at the carboxylic group at the 2 or 5-position have negative charges in the range of −0.01684 and −0.1693 e. So PEPE π-charges of thiophenes, which were substituted at the 2 and or 5-positions, show good agreement with the corresponding values of inhibition efficiency.

In conclusion, small changes in the S charge values strongly influence the degree of inhibition. TBCP shows extremely good inhibition (83%). An intramolecular

effect between phenylhydrazone and tertiobutoxy groups was observed.

The inhibition efficiency of thiophene compounds follows the sequence:

$$MTC(-27\%) < ETC(-11\%) < TM(12\%) < T(30\%)$$
$$< TBCA(37\%) < TBCP(83\%)$$

More information may be also obtained from the calculated quantum chemical indices like E_{HOMO}, E_{LUMO} and energy gap, $\Delta E = (E_{HOMO} - E_{LUMO})$. HOMO is the highest occupied molecular orbital and LUMO is the lowest unoccupied molecular orbital. Values of energies of LUMO and HOMO, ΔE and percent inhibition efficiencies, are given in Table 3.

E_{HOMO} is often associated with the electron donating ability of the molecule. High values of E_{HOMO} indicate a tendency of the molecule to donate electrons to appropriate acceptor molecules with low energy, empty molecular orbitals. Therefore, the energy of the lowest unoccupied molecular orbitals indicates the ability of the molecule to accept electrons. Also the less negative HOMO and the smaller energy gap are reflected in stronger chemisorption bond and perhaps greater inhibitor efficiency [24]. The plot of the inhibition efficiency of thiophenes against E_{HOMO} was linear with a slope close to unity and regression coefficient $R = 0.964$ (Figure 2).

Thus TBCP is the best inhibitor of the series studied and a detailed study was conducted.

The influence of TBCP concentration on the corrosion rate was determined (Table 4). The corrosiveness is markedly reduced with increasing inhibitor concentration. The highest inhibition efficiency 85% is observed at 5×10^{-3} M.

Figure 3 depicts the polarisation curves for steel in 0.5 M H_2SO_4 at different TBCP concentrations. Values of associated electrochemical parameters and corresponding inhibition efficiencies ($E\%$) are given in Table 5.

The addition of TBCP leads to a decrease in the cathodic current densities. The cathodic portions rise to Tafel lines indicating that the hydrogen evolution reaction is activation controlled. The addition of the inhibitor to the corrosive solution does not modify the cathodic Tafel slope β_c and the mechanism of the reduction process is not affected. The free corrosion potential determined after 30 min immersion does not change in the presence of the inhibitor. The polarisation curves for steel in H_2SO_4 show that the presence of

Table 2. Comparison of π-charges in thiophene derivatives calculated by PETRA program

	E/%	Calculation of π total charges/e				
		O(1)	S	O(2)	N(1)	N(2)
TBCA	37	0.0608	0.0173	−0.01856	–	–
TBCP	83	0.0532	0.0159	–	−0.0911	0.1581
T	30	–	0.0	–	–	–
ETC	−11	–	0.0285	0.1684	–	–
MTC	−27	–	0.0284	−0.1693	–	–
TM	12	0.0	0.0	–	–	–

Table 3. Quantum chemical calculations for the studied inhibitors

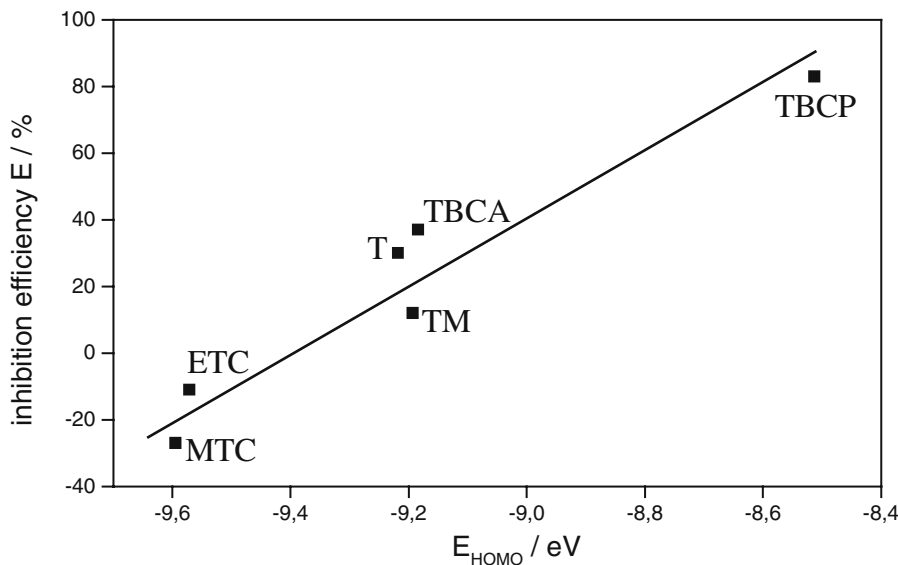| Compound 10^{-3} M	E_{HOMO}/eV	E_{LUMO}/eV	ΔE/eV	E/%
MTC	−9.595	−0.640	8.955	−27
ETC	−9.571	−0.610	8.961	−11
TM	−9.193	0.123	9.316	12
T	−9.218	0.238	9.546	30
TBCA	−9.184	−0.581	8.603	37
TBCP	−8.513	−0.307	8.206	83

Fig. 2. Correlation of HOMO energies with percent inhibition of thiophene derivatives.

Table 4. Steel weight loss data and corresponding inhibition efficiency of TBCP & at 298 K

Concentration/M	W_{corr}/mg cm^{-2} h^{-1}	E_w/%
Blank	1.608	–
TBCP		
10^{-5}	1.694	5
5×10^{-5}	1.603	00
10^{-4}	1.573	02
5×10^{-4}	0.811	49
10^{-3}	0.268	83
5×10^{-3}	0.236	85

TBCP inhibits only the cathodic process. This phenomenon is more pronounced with the concentration of inhibitor. E% values increase with inhibitor concentration and attains a maximum value of 87% at 5×10^{-3} M. In the anodic domain the curve characteristics are slightly modified in the presence of inhibitor. Then, TBCP acts essentially as cathodic inhibitor.

3.2. Effect of temperature

Corrosion reactions are usually regarded as Arrhenius processes and the rate (W) can be expressed by the relation:

$$\log(W) = \frac{-E_a}{RT} + A$$

where E_a is the activation energy of the corrosion process.

Gravimetric measurements were taken at various temperatures (298–353 K) in the presence and absence
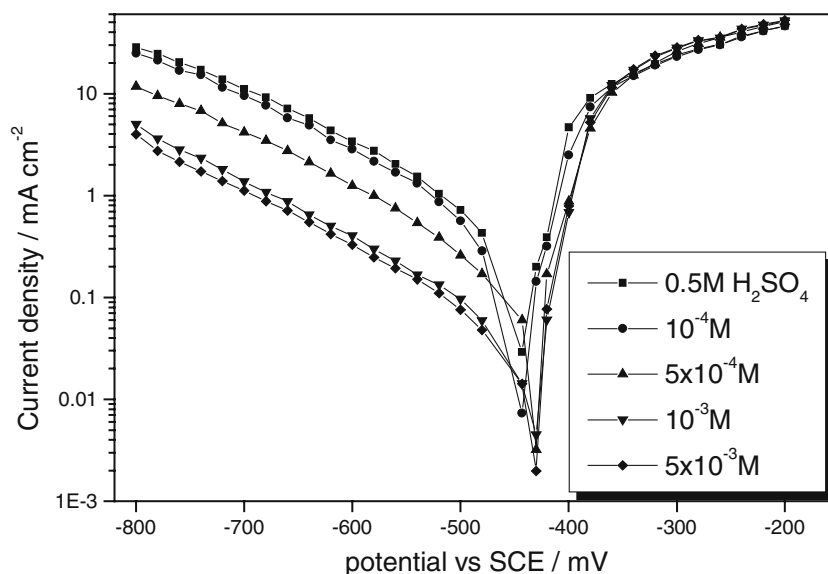

Fig. 3. Polarisation curves of steel in 0.5 M H$_2$SO$_4$ with and without TBCP at different contents.

Table 5. Electrochemical parameters of steel in H_2SO_4 at various concentrations of TBCP

Concentration/M	E_{corr} vs. SCE/mV	b_c/mV dec^{-1}	b_a/mV dec^{-1}	I_{corr}/μA cm^{-2}	E/%
Blank	−463	184	36	530	–
10^{-4}	−450	187	40	502	5
5×10^{-4}	−445	186	35	262	50
10^{-3}	−443	178	43	90	83
5×10^{-3}	−459	171	42	70	87

Table 6. Effect of temperature on the corrosion of steel with and without 5×10^{-3} M of TBCP

Temperature/K	W^0_{corr}/mg cm^{-2} h^{-1}	W_{corr}/mg cm^{-2} h^{-1} (TBCP)	E/%
298	0.149	0.991	85
303	0.165	1.182	86
313	0.470	3.135	85
323	0.808	6.182	87
333	1.905	12.70	85
343	2.850	19.00	85
353	4.662	33.30	86

of 5×10^{-3} M of TBCP at 1 h of immersion. The corresponding results are given in Table 6.

From these results, we can deduce that the corrosion rate increases in the blank with rise in temperature, but in the presence of TBCP, the dissolution is delayed. E% remains almost constant with increase in temperature.

Arrhenius plots for the corrosion of steel are given in Figure 4. The calculated values of activation energies in the presence and absence of TBCP were $E'_a = 57.5$ and $E_a = 57.7$ kJ mol^{-1}, respectively. The constancy in activation energy supports the results obtained by gravimetric and electrochemical studies and indicates

that TBCP is an efficient inhibitor and can be used in pickling baths.

3.3. *Electrochemical impedance spectroscopy measurements*

The corrosion behaviour of steel, in acidic solution in the presence of TBCP at different concentrations was investigated by EIS measurements at room temperature. The locus of Nyquist plots is regarded as one part of a semicircle. The equivalent circuit model employed for this system is as previously reported in the literature [25] and shown in Figure 5. Nyquist plots of steel in inhibited and uninhibited acidic solutions containing various concentrations of TBCP are shown in Figure 6. The charge transfer resistance, R_t, the double layer capacitance C_{dl} and the frequency f_{max} values are given in Table 7.

The semicircle in the impedance diagrams indicates that the corrosion of steel is controlled by a charge transfer process. Table 6 shows the impedance parameters obtained by line fitting to the semicircle. The charge transfer resistance (R_t) increases with the inhibitor concentration. Also, the double layer capacitance (C_{dl}) decreases with increase in the concentration of the inhibitor. This decrease is due to the adsorption of the inhibitor at the metal surface causing a change in the double layer structure [26]. When comparing the inhibition efficiencies obtained from testing methods used in this study, it can be concluded that there is a fair agreement between results obtained by the different techniques used.

3.4. *Adsorption isotherm*

Figure 7 shows the dependence of the fraction of the surface covered θ as a function of the logarithm of the TBCP concentration, where θ is the ratio E/100. The
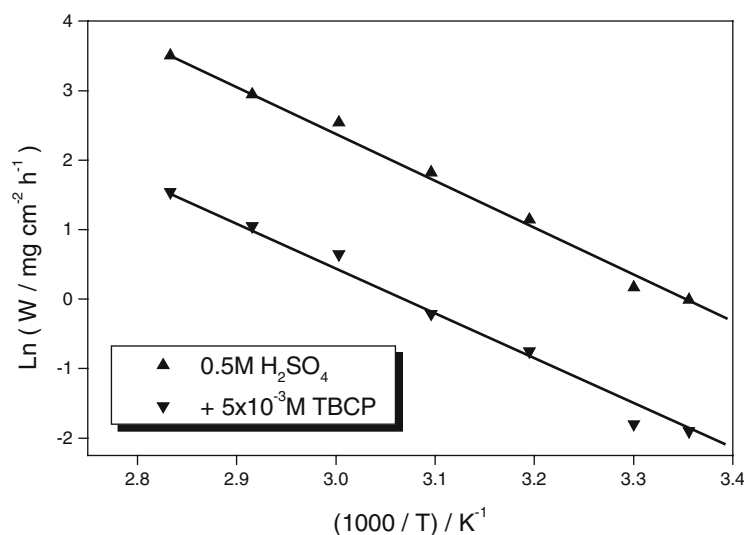

Fig. 4. Arrhenius plots for steel in 0.5 M H_2SO_4 with and without TBCP at 5×10^{-3} M.
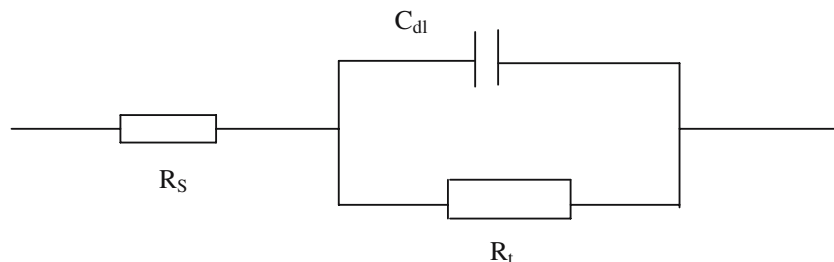
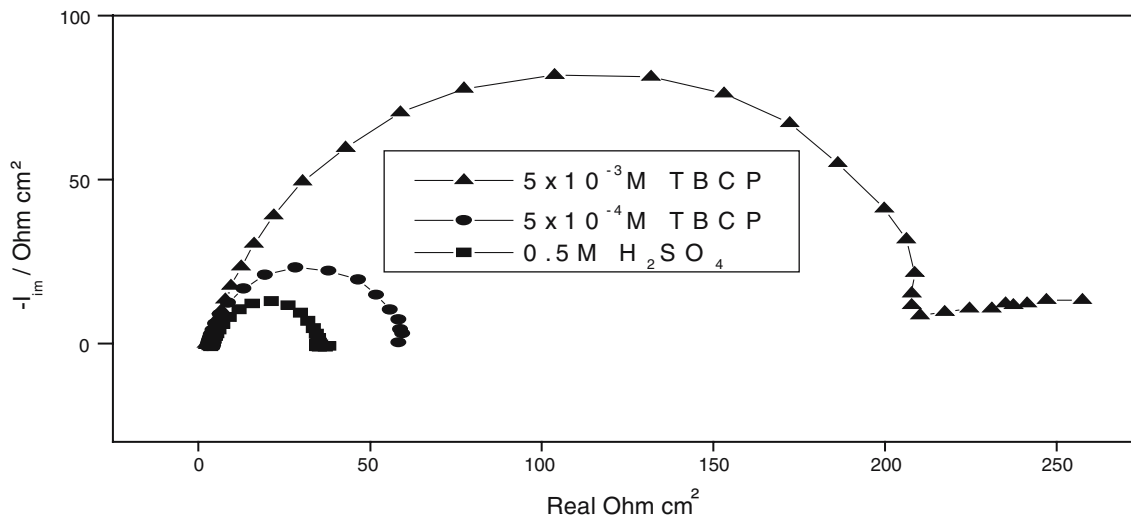*Fig. 5.* Equivalent circuit used in the modelling of the EIS data.

Fig. 6. Nyquist diagrams for steel in 0.5 M H_2SO_4 with different concentrations of TBCP.

Table 7. AC impedance data for steel in 0.5 M H_2SO_4 in presence and absence of TBCP

Concentration/M	R_t/Ω cm^2	f_{max}/Hz	C_{dl}/μF cm^{-2}	$E/\%$
blank	30	51.50	103	–
5×10^{-4}	58	35.31	77.70	48
5×10^{-3}	217	17.89	40.99	86

plot is consistent with a double S-shaped adsorbed isotherm showing adsorption according to the Frumkin isotherm [27]:

$$\left(\frac{\Theta}{1-\Theta}\right)\exp(-f\Theta) = \frac{1}{55.5}C\cdot\exp\left(\frac{-\Delta G_{ads}}{RT}\right)$$

f is a function of adsorption energy and ΔG_{ads} is a standard free energy of adsorption. Two values of concentration lead to the evaluation of f and ΔG_{ads} which were 4.59 and −42.7 kJ mol^{-1}, respectively. The negative value of ΔG_{ads} suggests that TBCP is spontaneously adsorbed on the metal surface [28]. Moretti et al. pointed out that when the value of ΔG_{ads} is more negative than −40 kJ mol^{-1}, chemisorption takes place by charge sharing or transfer from the organic molecule to the metal surface to form a co-ordinate type of bond [29]. The positive value of f indicates repulsion of inhibitor molecules at the surface. The S-shaped adsorption mode indicates that the mechanism of inhibition involves two possibilities of adsorption. At a very low concentration, the inhibitor is adsorbed at the metal surface in vertical mode. The plateau means that all the active sites on the surface are occupied by the inhibitor molecules forming a complete monolayer in horizontal mode. Further increase of inhibitor concentration leads to the formation of a multilayer structure [30]. The chemisorption mode may be represented by the scheme shown in Figure 8.

4. Conclusion

The inhibition efficiency of thiophene compounds may be classified as:

$$\text{MTC}(-27\%) < \text{ETC}(-11\%) < \text{TM}(12\%)$$
$$< \text{T}(30\%) < \text{TBCA}(37\%) < \text{TBCP}(83\%)$$

TBCP is an efficient inhibitor for steel in 0.5 M H_2SO_4.
The inhibition efficiency of TBCP attains a maximum value of 87% at 5×10^{-3} M.
It acts as a cathodic-type inhibitor without modifying the mechanism of hydrogen evolution.
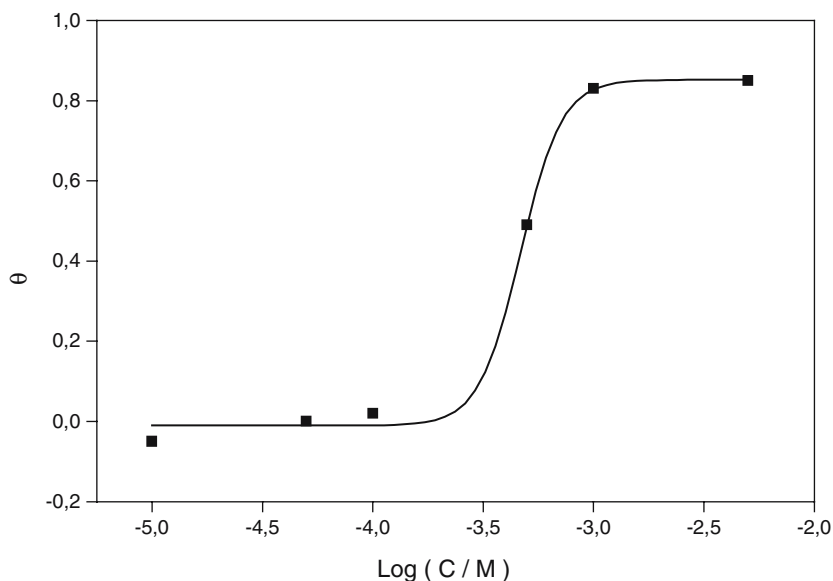The inhibition efficiency of TBCP is temperature independent.

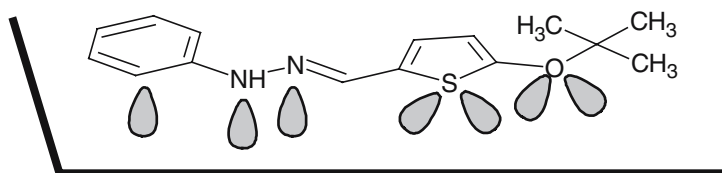*Fig. 7.* Isotherm adsorption model of TBCP on the surface of steel in 0.5 M H_2SO_4.

Fig. 8. Adsorption mode suggested of TBCP on the steel surface.

TBCP is adsorbed according to the Frumkin adsorption isotherm.

Acknowledgments

References

1. A. Popova, E. Sokolova, S. Raicheva and M. Christov, *Corros. Sci* **45** (2003) 33.
2. E.A. Noor, *Corros. Sci* **47** (2005) 33.
3. Sk.A. Ali, M.T. Saeed and S.U. Rahman, *Corros. Sci* **45** (2003) 253.
4. A. Chetouani, K. Medjahed, K.E. Sid-Lakhdar, B. Hammouti, M. Benkaddour and A. Mansri, *Corros. Sci* **46** (2004) 2421.
5. A. Dadgarnezhad, I. Sheikhshoaie and F. Baghaei, *Anti-Corros. Method. Mater.* **51** (2004) 266.
6. J.G.N. Thomas, in: 5th Europ. Symp. on Corrosion inhibitors, Ann. Univ. Ferrara, Italy, 1980 (1981) p. 453.
7. E. McCafferty, in: H.Leidheiser (Ed.), Corrosion Control by Coating (Science Press, Princeton, NJ, 1979), p. 279.
8. N. Hackerman and R. Hard, Proceed 1st Internat. Cong. Metal. Corros. (Butterworths, London, 1962) p. 166.
9. T. Tüken, B. Yazici and M. Erbil, *Prog. Org. Coat.* **51** (2004) 205.
10. L. Cheng, A.B. Bocarsly, S.L. Bernasek and T.A. Ramanarayanan, *Surf. Sci* **374** (1997) 357.
11. M.M. Abou-Romia and M.M. Hefny, *J. Electroanal. Chem.* **136** (1982) 339.
12. A.A. Samarkandy, A.O. Al-Oubi, R.M. Khalil and A.A. Abdel Fattah, *Bull. Electrochem.* **17** (2001) 111.
13. B. Mernari, L. El Kadi and S. Kertit, *Bull. Electrochem.* **17** (2001) 115.
14. K. Mori, Y. Okai, H. Horie and H. Yamada, *Corros. Sci* **32** (1991) 1237.
15. R.S. Sapieszko and E. Matijevi, *J. Colloid Interf. Sci.* **74** (1980) 405.
16. M.N.H. Moussa, F.I.M. Taha, M.A. Gouda M. and G.M. Singab, *Corros. Sci* **16** (1976) 379.
17. M. Broussely, J.C. Goudeau and M.L. Bernard, *Electrochim. Acta* **20** (1975) 233.
18. M.A. Elmorsi, M.M. Ghoneim, F.M. Issa and E.M. Mabrouk, *Surf. Coat. Technol.* **31** (1987) 389.
19. A. Galal, N.F. Atta and M.H.S. Al-Hassan, *Mater. Chem. Phys.* **89** (2005) 28 and 38.
20. S. Elayyoubi, E.B. Maarouf, H. Oudda and B. Hammouti, *Bull. Electrochem.* **18** (2002) 45.
21. A. Ouchrif, A. Yahyi, B. Hammouti, A. Dafali, M. Benkaddour and A. Et-Touhami, *Bull. Electrochem.* **19** (2003) 455.
22. M. Bouklah, B. Hammouti, A. Aouniti and T. Benhadda, *Prop. Org. Coat.* **47** (2004) 225.
23. W.-D. Ihlenfeldt and J. Gasteiger, *J. Comput. Chem.* **8** (1994) 793.
24. H.F. Finley and N. Hackerman, *J. Electrochem. Soc.* **107** (1960) 259.
25. F. Mansfeld, M.W. Kending and W.J. lorentz, *J. Electrochem. Soc.* **132** (1985) 290.
26. Z. Szklarska-smialowska, *Electrochemical and Optical Techniques for the study of Metallic Corrosion* (Kluwer Academic Publishers, Dordrecht, 1991), pp. 545.
27. A.N. Frumkin, *Z. Phys. Chem.* **116** (1925) 466.
28. J.D. Talati and D.K. Gandhi, *Corros. Sci.* **23** (1983) 1315.
29. G. Moretti, F. Guidi and G. Grion, *Corros. Sci.* **46** (2004) 387.
30. M.M. Osman and M.N. Shalaby, *Mater. Chem. Phys.* **77** (2002) 261.